Synthesis of SiO2 based nanocomposite of Agar and its characterization

Dinesh sen
(VIT-vellore , B.N.P.G. collage Udaipur.INDIA)

Abstract: *The newly developed Agar-SiO2 nanocomposite was prepared by hydrothermal method at room temperature. Such nanocomposites could be promising candidate for biomedical and environmental applications. Structural morphology was characterized using scanning electron microscopy (SEM) and Chemical interactions between SiO2 and Agar were analyzed using Fourier transform infrared spectroscopy equipped with attenuated total reflectance (FTIR-ATR), scanning electron microscopy-energy dispersive X-ray spectrophotometry (SEM-EDS) thermogravimetric analysis (TG) and differential scanning calorimetry (DSC). According to the TEM observation, the average composite granules size was about 60 nm and the embedded SiO2 nanoparticles were uniform with an average diameter of 25 nm*
Keywords: *Agar, Silicon dioxide, Characterization, TEM, Thermal properties.*

I. Introduction

Agar is a structural heteropolysaccharide contained in the primary cell walls of terrestrial plants which functions as an intercellular and intracellular cementing material. which forms the supporting structure in the cell walls of certain species of algae, and which is released on boiling. Agar has a very complex structure that depends on both its source and the extraction process. Its properties depend on its degree of esterification [10]. Agar is biodegradable, biocompatible and has also been reported to be bioactive [11]. Agar also contains the hydroxyl (-OH) functional group which enhances its chemical properties and carboxylic acid (-COOH) groups which permit direct bonding to SiO2.

Non-metal oxide based biocomposite have been attracting significant attention due to their various potential applications in catalysis, electronics, photonics, and sensors [1–8].Agar is commonly used in the food industry as a gelling and stabilizing agent. Agar macromolecules are able to bind with some organic or inorganic substances via molecular interactions. So, Agar can be used to construct matrices to absorb desired materials and deliver them in a controlled manner [9].

The core principle of this concept is to use biopolymers which are chemically and thermally stable under very specific conditions *in vitro*. Thus, the goal of extreme biomimetics is to bring together broad variety of solvo-thermal and hydrothermal synthesis reactions with templates of biological origin for the generation of novel hybrid composites

In addition to alumina, silica, and titania, silica has been gaining tremendous importance mainly due to its enhanced reactivity and optical properties [12, 13].Silicon oxide nanoparticles have attracted much attention in nanotechnology and recent materials science, as SiO2 possesses unique physicochemical properties attractive for specific and advanced applications. It exhibits high values for its dielectric constant, refractive index, thermal stability and mechanical strength [14].

Herein, we report the preparation of Agar-SiO2 nanocomposite with a facile solution approach at room temperature. This approach may find potential application in the food industry. Intriguingly, there are only few references regarding the use of biological templates for forming the desired phases of Silicon oxide. These only relate to the formation of germania nanoparticles and principally, no papers seem to exist on the development of germania-based biocomposites

Thus far, several different technologies have been developed for synthesis of Silicon oxide with these desired properties; including sol-gel reactions [15-18], thermal evaporation [19] reverse micelle method [20], direct precipitation followed by calcination [21, 22] as well as thermal oxidation [23, 24].

II. Experimental

2.1Materials
Agar from apples was purchased from Sigma Aldrich in powder form. The molecular weight of Agar was in the range 33,000–100,000 and the degree of esterification was about 65–70%, on a dry basis, total impurities ≤ 10% water. Silicon dioxide was used as received. All other chemicals, solvent and indicators were of analytical grade (Thomas Baker, India). Doubly distilled water was used for all the experiments.

2.2 Method

For a typical synthesis, 1 g SiO2, 0.30 g Agar and 50 mL distilled water were added into a 100 mL beaker. After full dissolution, 50 mL of 0.300 M NaOH solution was added dropwise under constant stirring. The reaction was allowed to proceed at room temperature (25 ^{o}C) for 24 h. Then, the obtained white precipitate was centrifuged at 10,000 rpm for 15 min and collected and washed with distilled water several times to remove the byproducts. After drying in vacuum at 30 ^{o}C for 6 h, the final product was obtained as white-yellow powder.

2.3 Characterization

The infrared spectra for identifying the functional groups and the existence of halogen bonding were recorded using a Perkin Elmer 2000 FT-IR spectrometer with a horizontal attenuated total reflection (ATR) cell (USA). The ATR diamond crystal was carefully cleaned with pure isopropyl alcohol. About 10 mg of powdered sample was carefully placed on the diamond crystal surface, and the spectrum was recorded as transmittance under 100 N. The spectrum was scanned between 3600 and 600 cm^{-1} at a resolution of 4 cm^{-1}.

A plot between weight loss and temperature was recorded in thermogravimetric analysis (TGA) using Pyris-1 (Perkin–Elmer, Shelton, USA). Initially, the sample (about 6 mg) was placed under nitrogen atmosphere (flow rate 25 mL/min); then the gas was changed to oxygen (flow rate 35 mL/min) and heating continued up to 700 ^{o}C with heating rate at 10 ^{o}C per minute. DTG was performed at 10 ^{o}C, which gives the decomposition temperature. Phase transitions were investigated over the range of 300–250 ^{o}C in N_2 atmosphere using a Perkin–Elmer diamond differential scanning calorimetry (DSC). A plot between enthalpy change and temperature was obtained at heating rate of 10 ^{o}C per minute.

Energy dispersive X-ray spectrophotometry study was carried out with the help of Quantax 200 with X-Flash liquid nitrogen free detector from Bruker, Germany for the elemental mapping of the samples. For transmission electron microscopy measurements, 100 nm sections were microtomed at 21208C using Ultracut E ultramicrotome (Reichert and Jung) with a diamond knife. Measurements were carried out with a Philips CM200 TEM at an acceleration voltage of 120 kV.

III. Results and Discussion

Agar is a polysaccharide that acts as a cementing material in the cell walls of all plant tissues manufacturing of Agar is done in winter. The red algae are grown in the sea, on the support of poles on, which they develop. These poles are withdrawn, algae is removed, dried, beaten and shaken to remove shell and sand. The algae are bleached by exposure to sun light or washing with water.

The washing with water removes the associated salts. Then these are boiled with acidulated water (one part algae with 55- 60 parts water) for few hours. Mucilaginous mass is filtered while hot then cooled. The jelly is formed and cut into bars. These bars are forced through wire netting and strips are formed. These are dried in sunlight and freezing and thawing remove moisture. Finally, agar is dried at 35°C. A neutral galactose polymer. It is free from sulphate. The gel strength of agar is due to this component. Agarose also called as Agarobiose is a disaccharide consisting alternate residues of 1, 4-α-linked 1, 3-β-D galactose and 3, 6-anhydro-L-galactose. While the disaccharide unit is called agarobiose or neoagarobiose, the linear chain is called agarose. An acidic sulphonated component where in 1, 3 linked D-galactose and the galactouronic acid (an uronic acid) are partly esterified with sulphuric acid. Agaropectin comprises 90% and more of sulphur. In addition, the sulphate group may also get linked to calcium, magnesium, potassium or sodium.

. The Degree of Esterification (DE) affects the gelling properties of Agar. The structure shown here has three methyl ester forms (**-COOCH₃**) for every two carboxyl groups (**-COOH**), hence it is has a 70% degree of esterification, normally called a DE-70 Agar.

3.1 FT-IR study

The formation of the Agar–Silicon dioxide nanocomposite powders was also confirmed by IR spectroscopy. FTIR spectrum of pure Agar confirmed by in the wavelength range of 950 and 1200 cm^{-1} are considered as the 'finger print' region for carbohydrates as it allows the identification of major chemical groups in polysaccharides [25]. This region is dominated by ring vibrations overlapped with stretching vibrations of (C-OH) side groups and the (C-O-C)

glycosidic bond vibration. bands at 1100 and 1017 cm^{-1} were strongest, similarly as reported earlier[26,27]. The unique spectral shape of Agar is due to the high homogalacturonan content and Agar has linked backbones. Agars DE were determined using the peak area relation of the free carboxyl groups (1650 cm^{-1}) and esterified groups (1750 cm^{-1}) [28]. Also peaks found at 890 and 960 cm^{-1} were assigned to Ge–O–Ge (the antisymmetric stretching mode of hexagonal SiO2) [29-31]. and a short peak at 1100 cm^{-1}, which correspond to Si–O–Si [32] the two new peaks at 1458 cm-1 and 1376.4 cm−1 have been attributed to the symmetric and asymmetric stretching of carboxylate-nonmetal linkage [33, 34].

3.2 SEM-EDS study

SEM-ESD images of Agar-SiO2 nanocomposites shown in Fig. 1 SEM images of Agar-SiO2 nanocomposites exhibited the rough surface with granular morphology. SEM image indicated the binding of Agar with SiO2. It has been inferred that the size and the homogeneity of particles dependent on the binding of biopolymer with inorganic counterpart. EDX shows that the composite composed of carbon, Silicon, calcium and oxygen with 17.85%, 78.50, 2.12 and 14.51 percentage, respectively (Fig.2 and Table 1).

3.3 SEM and TEM study

The SEM image in Fig.3 (a) shows that the polymeric nature of the Agar remained intact during the synthesis. There is no agglomeration of the particles indicating that the Agar coated the Silicon oxide nanoparticles. SEM images also revealed that the pores of the composite were often smaller than the alone, and they were always lined or bordered by smooth, leaf-like surfaces. These surfaces resembled the appearance of the image texture of isolated Agar particles used to make the composite. Nevertheless, it is difficult to localize the SiO2 based on image features alone.

Transmission electron microscopy (TEM) studies of Agar-SiO2 nanocomposites were carried to study the particle size. In this, suspension of material was prepared in ethanol onto a carbon copper grid. TEM produces high resolution, black and white images from the interaction between samples and energetic electrons in the vacuum chamber. TEM provides topographical, morphological, compositional and crystalline information.

A typical TEM image of the Agar–SiO2 nanocomposite is shown in Fig.3 (b). TEM image shows the dispersed homogeneous particles with diameters of around 20 nm. The different contrast on every particle indicates its different composition and structure. The dark part is Agar wrapped SiO2 and the gray part is Agar (diameters of around 70 nm).

3.4 Thermal study

The TG curve records the weight loss during heating and the DSC curve describes changes in the reaction enthalpy during the degradation. The differential thermogravimetry (DTG) curve is the first derivation of the TG curve and reports the degradation velocity. The TG and DTG thermogram Agar-GeO$_2$ nanocomposite analysis is depicted in Fig.4 It exhibits two stage decomposition processes. The first stage decomposition ($T_d = 61$ ^{o}C) may be due to expulsion of water molecules present in the Agar-SiO2 nanocompostes. In the second stage decomposition (768 ^{o}C) corresponds to the loss of side group elimination attached and due to main chain scission.

By contrast, in the DSC curve, only one thermal event, endothermic, are clearly distinguished up to 250°C (Fig. 5). In broad strokes, these thermal events are related to dehydration and thermal degradation processes, including the depolymerization degree at different stages as well as the secondary decomposition stage of Agar present in Agar –Silicon dioxide nanocomposite. However, according to the DSC curve, this broad thermal event (endothermic) at 99.8 ^{o}C (with area swept in endotherm 276.4 mJ and enthalpy change (48.1 J/g) can be identified. This suggests the presence of at least two weakly bonded water types, namely physically adsorbed water interacting only with other water molecules and those involved in hydrogen bonds with Agar hydroxyl groups.

IV. Conclusion

This paper reported the fabrication of new Agar-SiO2 nanocomposites for possible applications new semiconducting material for electronic applications. This synthesized material was characterized by FTIR, SEM-EDX, TEM, TG-DTG and DSC. TEM results indicated the particle size in the range between 20 nm and 70 nm. Therefore, the newly synthesized Agar-SiO2 nanocomposite can be used as potential material for environmental friendly electronic materials.

References

[1]. Zheng, X., Wang, H. and Xu, B.Q. *J. Phys. Chem. B*, **2005**, 108(19): 9678.
[2]. Gong, K.; Yu, P.; Su, L.; Xieng, S. and Mao, L. *J. Phys. Chem. C,* **2007**, 115(5): 1882.
[3]. McCue, J.T. and Ying, J. Chem. Mater. **2007**, 19(5): 1009.
[4]. Guo, J., She, C. and Lian, T. *J. Phys. Chem. C*, **2008**, 112(12), 4761.
[5]. Xu, Z.; Xu, R. and Zeng, H.C. *Nano Lett.* **2001**, 1(12), 703.
[6]. Liu, L.S.; Cooke, P.H.; Coffin, D.R.; Fishman, M.L. and Hicks K.B. *J. Appl. Polym. Sci.* **2004**, 92, 1893. Tomaev, V.; Mosnikov, V.; Miroshkin, V.; Garkin, L.; Yu, A. and Zhivago, S. *Glass Physics Chem.* **2004**, 10, 461.
[7]. ßtefania, Silvia, V.; Marcel P. and Cornelia, L. *Revue Roumaine de Chimie*, **2009**, 54,(9) 709.
[8]. Sharma, B. R.; Naresh, L.; Dhuldhoya, N. C.; Merchant, S. U. and Merchant U. C., *Times Food Processing Journal*, **2006**, 23 (2), 44.
[9]. Verelst, M., Ely, T.O.; Amiens, C.; Snoeck, E.; Lecante, P.; Mosset, A.; Respaud, M.; Broto, J.M. and Chaudret, B. *Chem. Mater.* **1999** , 11(10), 2702.
[10]. Rimer, J.; Roth, D.; Vlachos, D. and Lobo, R. *Langmuir*, **2007**, 23, 2784.

[11]. Ramana, C. V.; Carbajal-Franco, G.; Vemuri, R. S.; Troitskaia, I. B.; Gromilov, S. A.; Atuchin, V. V. *Mater. Sci. Eng. B* **2010**, 174, 279. Limthongkul, P.; Wang, H. and Chiang, Y.M. *Chem. Mater.* **2001**, 13(7): 2397 Wu, X.; Song, W.H.; Zhao, B.; Sun, Y. and Du, J. *Chem. Phys. Lett.,* **2001**, 349 : 210.
[12]. Liu, L.S.; Cooke, P.H.; Coffin, D.R.; Fishman, M.L. and Hicks K.B. *J. Appl. Polym. Sci.* **2004**, 92, 1893. Tomaev, V.; Mosnikov, V.; Miroshkin, V.; Garkin, L.; Yu, A. and Zhivago, S. *Glass Physics Chem.* **2004**, 10, 461.
[13]. Javadi, M.; Yang, Z.; Veinot,J. G. C. *Chem. Commun.* **2014**, 50, 6101.
[14]. Laubengayer, A. W.; Brandt, P. L. *J. Am. Chem. Soc*. **1932**, 54, 549.
[15]. Jiang, Z.; Xie, T.; Wang, G. Z.; Yuan, X. Y.; Ye, C. H.; Cai, W. P.; Meng, G. W.; Li, G. H.; Zhang, L. D. *Mater. Lett.* **2005**, 59, 416.
[16]. Wu, H. P.; Liu, J. F.; Ge, M. Y.; Niu, L.; Zeng, Y. W.; Wang, Y. W.; Lv, G. L.; Wang, L. N.; Zhang, G. Q.; Jiang, J. Z. *Chem. Mater* **2006**, 18, 1817.
[17]. Ramana, C. V.; Troitskaia, I. B.; Gromilov, S. A.; Atuchin, V. V. *Ceram. Int.* **2012**, 38, 5251. Krishnan, V.; Gross, S.; Müller, S.; Armelao, L.; Tondello, E.; Bertagnolli, H. *J. Phys. Chem. B* **2007**, 111, 7519
[18]. Atuchin, V. V; Gavrilova, T. A.; Gromilov, S. A.; Kostrovsky, V. G.; Pokrovsky, L. D.; Troitskaia, I. B.; Vemuri, R. S.; Carbajal-Franco, G.; Ramana, C. V *Cryst. Growth Des.* **2009**, 9, 1829. Jang, J.; Koo, J.; Bae, B.-S. *J. Am. Ceram. Soc.* **2000**, 83, 1356.
[19]. Gunji, M.; Thombare, S. V; Hu, S.; McIntyre, P. C. *Nanotechnology* **2012**, 23, 385603.
[20]. Cernà, M.; Barros, A.S.; Nunes, A.; Rocha, S.M.; Delgàdillo, I.; Copìkovà, J.; Coimbra, M.A. *Carbohydr. Polym.* **2003**, *19*, 793.
[21]. Coimbra, M. A., Barros, A., Barros, M., Rutledge, D. N.; Delgadillo, I. *Carbohydrate Research*, **1999**, 317, 145. Shinde, S. L.; Nanda, K. K. *Cryst Eng Comm* **2013**, 15, 1043.
[22]. Wellner, N., KacÆuraÂkova Â, M.; MalovõÂkova, Â, A.; Wilson, R. H.; Belton, P.
[23]. Gnanasambandan, R.; Proctor, A. *Food Chem.* **2000**, *68*, 327.
[24]. Lippincott, E. R.; Valkenburg, A. Van; Weir, C. E.; Bunting, E. N. *J. Res. Natl. Bur. Stand.*
[25]. Boix, E.; Puddu, V.; Perry, C. C. *Dalt. Trans.* **2014**, 43, 16902. S. *Carbohydrate Research*, **1998**, 308, 123..
[26]. Jing, C.; Hou, J.; Xu, X. *Opt. Mater.* **2008**, 30, 857.
[27]. Lipinska-Kalita, K.E. J. Non Cryst. Solids, **1990**, 119(1), 41. **1958**, 61, 61.
[28]. Gong, J.-L.; Wang, X.-Y.; Zeng, G.-M.; Chen, L.; Deng, J.-H.; Zhang X.-R.; Q.-Y. Niu,
[29]. Liu J.-F.; Shan, Z.; Zhao, H; Jiang, G.-B. *Environ- mental Science and Technology*, **2008**, 42, 18, 6949.
[30]. *Chemical Engineering Journal*, **2012**, 185-186,100.

Table 1. SEM-EDS data for Agar-SiO2 nanocomposite

Element	Series	unn. C [wt.-%]	Cnorm. C [wt.-%]	Atom. C [at.-%]	Oxide	Oxid. C [wt.-%]	Error [%]
Carbon	K-series	4.44	4.85	9.21	CO2	16.85	2.3
Sodium	K-series	0.83	0.13	0.16	Na2O	0.66	0.4
Chlorine	K-series	1.52	1.13	0.64	Cl	1.08	0.2
Silicon	K-series	39.45	45.69	16.57	SiO2	78.40	1.7
Calcium	K-series	1.22	1.52	0.74	CaO	2.52	0.2
Oxygen	K-series	46.65	43.68	72.38	O	14.11	6.5
Total:		97.70	100.00	100.00			
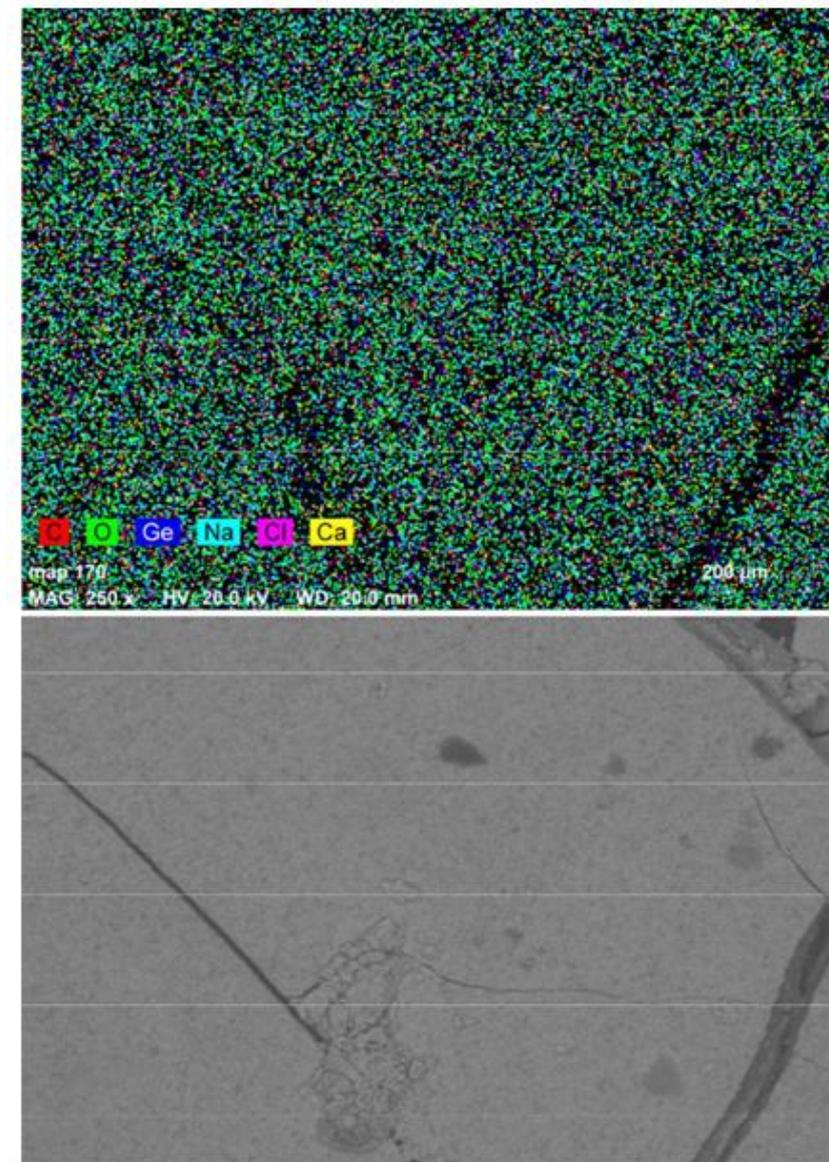
Fig. 1 SEM –EDS of Agar-SiO2 nanocomposite
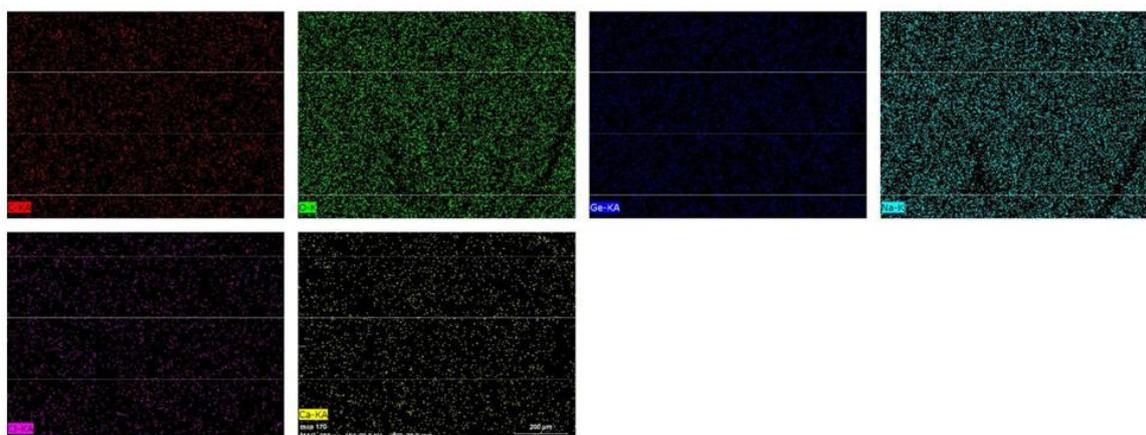
Figure 1(b) Al mapping of the various components present in Agar -SiO2 nanocomposite by EDS
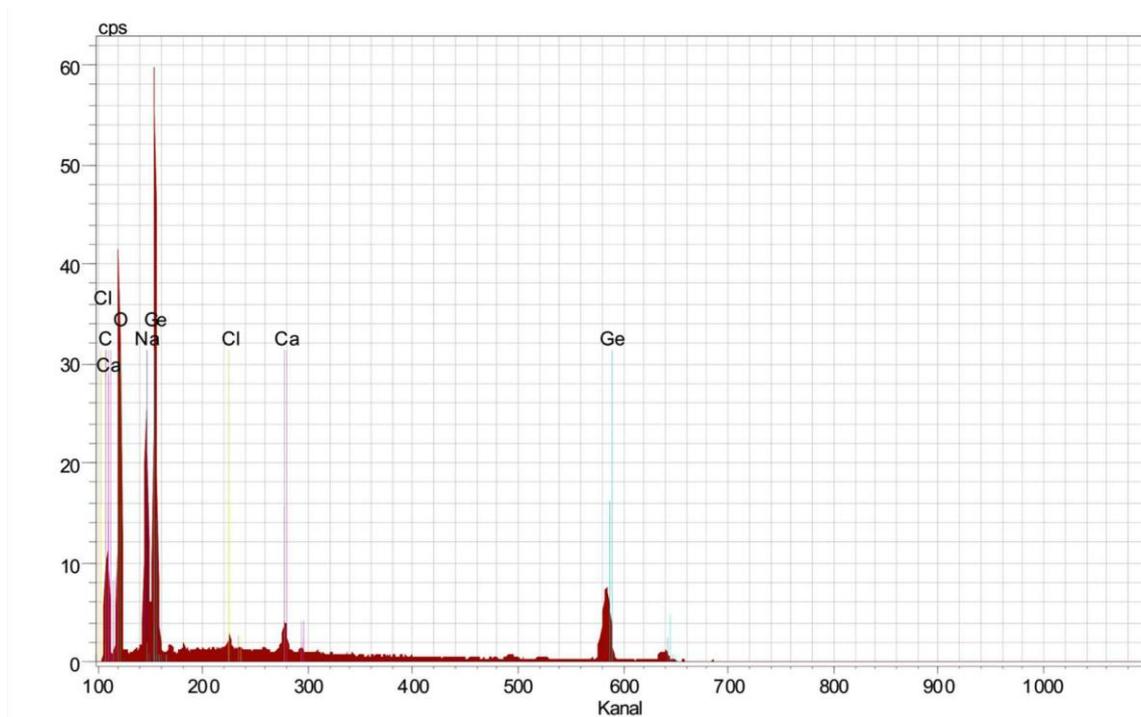
Fig. 2 EDS energy dispersive X-ray spectrum for Agar-SiO2 nanocomposite
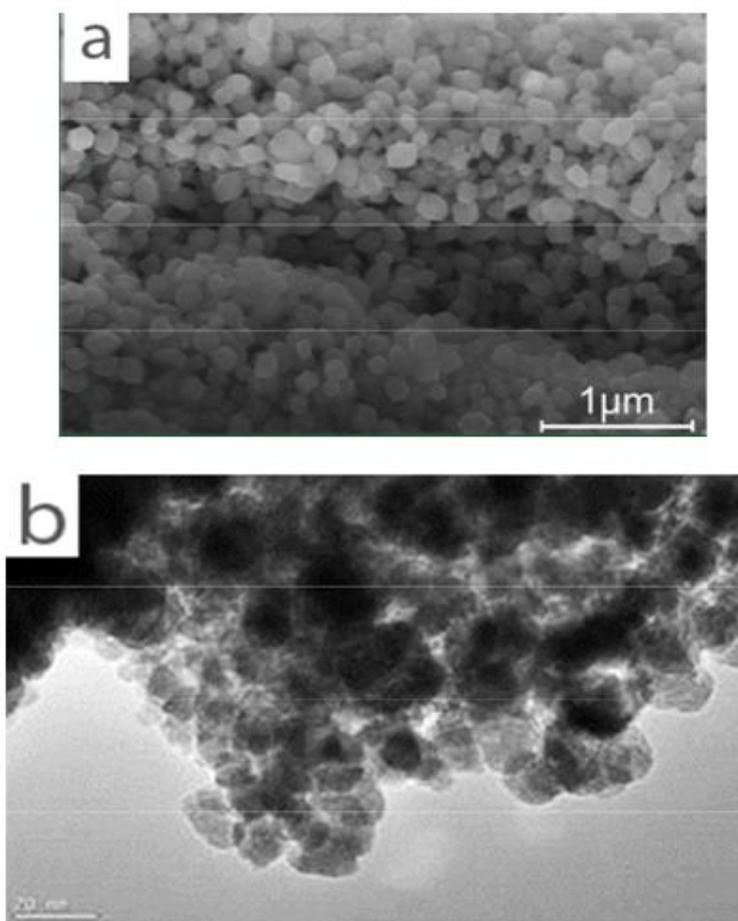
Fig. 3 (a) SEM (b) TEM images for Agar-SiO2 nanocomposite
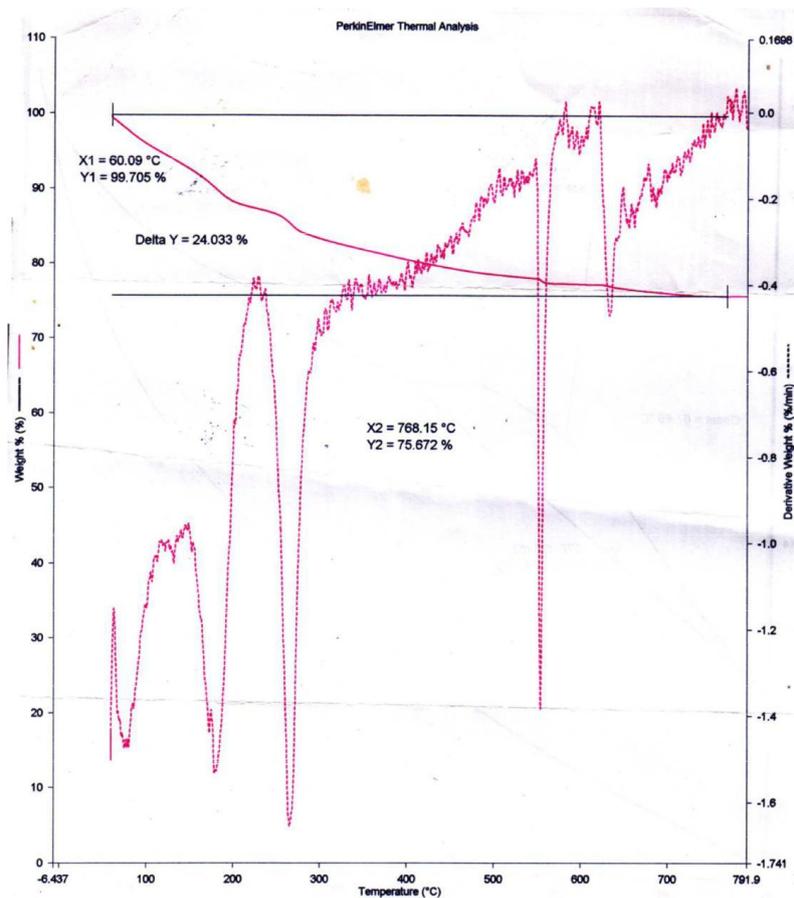
Fig.4 TG-DTG thermogram for Agar-SiO2 nanocomposite

Fig.5 TG-DTG thermogram for Agar-SiO2 nanocomposite